Thiocyanate binding to the molybdenum centre of the periplasmic nitrate reductase from *Paracoccus pantotrophus*

Clive S. BUTLER*[1], John M. CHARNOCK†‡, C. David GARNER§, Andrew J. THOMSON‖, Stuart J. FERGUSON¶, Ben C. BERKS‖ and David J. RICHARDSON‖

*School of Biochemistry and Genetics, Medical School, University of Newcastle, Newcastle upon Tyne NE2 4HH, U.K., †Department of Chemistry, University of Manchester, Manchester M13 9PL, U.K., ‡C.L.R.C. Daresbury Laboratory, Warrington WA4 4AD, U.K., §School of Chemistry, University of Nottingham, University Park, Nottingham NG7 2RD, U.K., ‖Centre for Metalloprotein Spectroscopy and Biology, University of East Anglia, Norwich NR4 7TJ, U.K., and ¶Department of Biochemistry, University of Oxford, South Parks Road, Oxford OX1 3QU, U.K.

The periplasmic nitrate reductase (NAP) from *Paracoccus pantotrophus* is a soluble two-subunit enzyme (NapAB) that binds two haem groups, a [4Fe–4S] cluster and a bis(molybdopterin guanine dinucleotide) (MGD) cofactor that catalyses the reduction of nitrate to nitrite. In the present study the effect of KSCN (potassium thiocyanate) as an inhibitor and Mo ligand has been investigated. Results are presented that show NAP is sensitive to SCN^- (thiocyanate) inhibition, with SCN^- acting as a competitive inhibitor of nitrate ($K_i \approx 4.0$ mM). The formation of a novel EPR Mo(V) species with an elevated g_{av} value ($g_{av} \sim 1.994$) compared to the Mo(V) High-*g* (resting) species was observed upon redox cycling in the presence of SCN^-. Mo K-edge EXAFS analysis of the dithionite-reduced NAP was best fitted as a mono-oxo Mo(IV) species with three Mo–S ligands at 2.35 Å (1 Å = 0.1 nm) and a Mo–O ligand at 2.14 Å. The addition of SCN^- to the reduced Mo(IV) NAP generated a sample that was best fitted as a mono-oxo (1.70 Å) Mo(IV) species with four Mo–S ligands at 2.34 Å. Taken together, the competitive nature of SCN^- inhibition of periplasmic nitrate reductase activity, the elevated Mo(V) EPR g_{av} value following redox cycling in the presence of SCN^- and the increase in sulphur co-ordination of Mo(IV) upon SCN^- binding, provide strong evidence for the direct binding of SCN^- via a sulphur atom to Mo.

Key words: EPR spectroscopy, EXAFS spectroscopy, ligand binding, molybdoenzymes.

INTRODUCTION

Three distinct classes of enzyme catalyse the bacterial reduction of nitrate to nitrite. Two of these enzymes are associated with energy-conserving respiratory electron-transport pathways and one with nitrate assimilation [1]. One of the respiratory enzymes is membrane-anchored, with an active site in the cytoplasm, and the other is a water-soluble periplasmic enzyme [2]. The assimilatory enzymes are located in the cytoplasm [1]. Sequence analysis has led to the conclusion that all the bacterial nitrate reductases are members of the subgroup of molybdoenzymes that bind the molybdopterin guanine dinucleotide (MGD) form of the molybdopterin cofactor [2]. The soluble periplasmic nitrate reductase (NAP) from *Paracoccus pantotrophus* (previously classified as *Thiosphaera pantotropha* [3] and *Paracoccus denitrificans* GB17) contains a 16 kDa dihaem *c*-type cytochrome subunit (NapB) and an 80 kDa catalytic subunit (NapA) that binds an N-terminal [4Fe–4S] cluster and the MGD cofactor [2,4–6]. NapA exhibits a high degree of sequence similarity to the MGD-binding polypeptides of bacterial assimilatory nitrate reductases (NAS) and formate dehydrogenases, both of which also bind an N-terminal iron–sulphur cluster and MGD [2,7]. NAP and NAS are quite distinct from the membrane-bound nitrate reductase (NAR), which is a three-subunit enzyme consisting of an integral membrane di-*b*-haem cytochrome, a water-soluble electron-transferring subunit that binds four iron–sulphur clusters and a large 140 kDa catalytic subunit that binds the MGD cofactor [2].

The crystal structure of monomeric NapA from *Desulfovibrio desulphuricans* has been reported recently [8] and has revealed the presence of two MGD moieties per polypeptide (bis-MGD). This is consistent with crystal structures of three other members of the MGD family, namely the soluble periplasmic dimethyl sulphoxide reductases (DMSOR) from *Rhodobacter capsulatus* and *R. sphaeroides*, the soluble formate dehydrogenase H from *Escherichia coli*, and the periplasmic trimethylamine *N*-oxide reductase (TMAO) from *Shewanella massilia* [9–13]. These two MGD moieties can provide up to four thiolate ligands to the Mo, although in the case of one structure of the DMSOR the dithiol of one MGD moiety is not co-ordinated to the Mo atom [10]. This indicates some flexibility in the catalytic site and this is reflected in a number of different Mo(V) EPR signals observed for these enzymes [14,15]. The most common and best documented change in the Mo co-ordination sphere that gives rise to EPR g_{av} value shifts is variation in the number of sulphur ligands and a correlation between increasing sulphur co-ordination and increasing g_{av} is evident from model compound studies [16,17]. Release of a pterin dithiol from the Mo co-ordination sphere may account for the decrease in g_{av} observed under certain reducing conditions in both NAP [15] and DMSOR [14]. Unusual Mo(V) signals with very high g_{av} values (> 2.00) are observed in the assimilatory nitrate reductases of *Azotobacter vinelandii* [18] and *Synechococcus* sp. (L. M. Rubio, C. S. Butler, D. J. Richardson, B. C. Berks, E. Flores and A. Herrero, unpublished work) and can also be generated in NAP by redox cycling in the presence of cyanide [15]. In this case, cyanide is a

Abbreviations used: MGD, molybdopterin guanine dinucleotide; NAP, periplasmic nitrate reductase; NAR, membrane-bound nitrate reductase; NAS, assimilatory nitrate reductase; DMSOR, dimethyl sulphoxide reductase; TMAO, periplasmic trimethylamine *N*-oxide reductase; MV^+, Methyl Viologen radical.

[1] To whom correspondence should be addressed (e-mail c.s.butler@ncl.ac.uk).

non-competitive inhibitor of NAP and does not bind at the Mo atom [15]. EXAFS analysis supports this observation and shows that the binding of cyanide somewhere in the active-site pocket causes a change in the Mo co-ordination geometry. This results in a significant distortion of the bond lengths of the co-ordinating sulphur ligands that may then lead to an increase in the observed g_{av}.

In order to understand how the different spectroscopic properties of these molybdopterin enzymes are related to changes in sulphur co-ordination, it is clearly important to study the effect of binding exogenous sulphur ligands. Furthermore, novel Mo-containing enzymes that have been implicated in the reduction of tetrathionate and thiosulphate have been identified recently [19]. The Mo cofactor within these enzymes acts as a sulphur-atom transferase by catalysing a reductive cleavage of a sulphur–sulphur bond [19] – a previously unrecognized function of the molybdopterin cofactor in biology. Consequently, this has generated further interest in the interaction of Mo with exogenous sulphur-containing ligands. In the present paper we have investigated the effect of KSCN (potassium thiocyanate) on the periplasmic nitrate reductase from *P. pantotrophus* as both a catalytic inhibitor and as a potential ligand of the Mo. The effects of SCN^- (thiocyanate) on the activity, EPR and EXAFS of NAP are discussed in the context of this anion binding directly to Mo through its sulphur atom.

EXPERIMENTAL

Purification and activity assays

P. pantotrophus M6 was grown anaerobically on nitrate and the NapAB complex purified as described by Berks et al. [5]. Enzyme activity was measured using reduced Methyl Viologen (MV^+) as electron donor as described previously [20]. Under these conditions, turnover was not re-reduction-limited [15], thus permitting the inhibitory effect of SCN^- on NAP to be measured.

Preparation of NAP SCN^- samples for EXAFS and EPR spectroscopy

Periplasmic nitrate reductase ($\approx 300\ \mu M$) in 20 mM Hepes buffer, pH 7.2, was reduced with a 50-fold excess of dithionite and incubated at room temperature for 10 min. KSCN (Sigma) was added to a final concentration of 10 mM, incubated for 10 min at room temperature and frozen under liquid nitrogen. For the EPR sample, ferricyanide was added (3 mM) to generate the Mo(V) EPR-detectable species.

EPR spectroscopy

EPR spectroscopy was performed on an X-band ER200-D spectrometer (Bruker Spectrospin; Bruker, Karlsruhe, Germany) interfaced to an ESP1600 computer and fitted with a liquid-helium-flow cryostat (ESR-9; Oxford Instruments, Oxford, U.K.). Mo(V) EPR spectra were recorded at 60 K, ≈ 9.64 GHz microwave frequency, 2 mW microwave power and 0.1 mT field modulation amplitude. Spin concentration of samples was determined from integrations of their EPR absorption spectra by comparison with those of a 2 mM Cu^{II}-EDTA standard as described previously [21].

EXAFS spectroscopy

Mo K-edge X-ray absorption spectra were recorded in fluorescence mode on frozen solutions at ≈ 10 K on the 6T-wiggler magnet beam-line, station 16.5 of the Synchrotron Radiation Source at the Daresbury Laboratory, Warrington, Cheshire, U.K., operating at 2 GeV with an average current of 150 mA. An Si(311) double crystal monochromator was used, with a vertically focusing mirror, which removed higher harmonics. The fluorescence was monitored using a liquid-nitrogen-cooled solid-state 30-element Canberra detector. The monochromator was calibrated at the start of run using an Mo foil, setting the position of the first peak of the derivative of the foil edge to 19999 eV. During multiple scanning of the sample, the edge position did not vary. Each spectrum was collected over ≈ 45 min.

Analysis of EXAFS data

The raw data were summed using the Daresbury program EXCALIB, and background subtraction was performed using EXBACK. The isolated k^3-weighted EXAFS data were analysed using EXCURV98 [22], employing the single-scattering spherical wave approximation [23,24]. Phaseshifts were derived from *ab initio* calculations using Hedin–Lundqvist potentials and von Barth ground states [25]. The theoretical fits were obtained by adding shells of backscattering atoms around the central absorber atom and refining the absorber-scatterer distances, r, the Debye–Waller type factor, $2\sigma^2$, and the Fermi energy correction, E_f, to get the best agreement with the experimental data.

RESULTS

Effect of SCN^- on NAP enzyme kinetics

NAP was assayed using MV^+ as electron donor and nitrate as electron acceptor [20]. Under these assay conditions NAP is incubated for approx. 2 min prior to the addition of oxidant. From the dependency of the maximum rate on nitrate concentration, a K_m of ~ 1.0 mM and k_{cat} of $\sim 250\ s^{-1}$ was calculated, these values are consistent with those published previously [15]. NAP in turnover was demonstrated to be sensitive to inhibition by KSCN when added at concentrations > 1 mM. The double-reciprocal ($1/v$ versus $1/[S]$) plot for SCN^- inhibition (Figure 1) shows clearly that SCN^- displays competitive

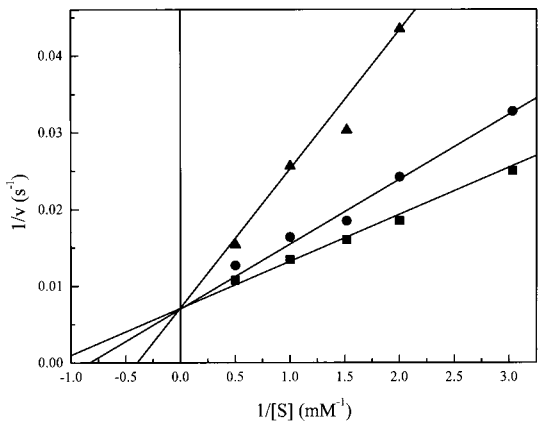

Figure 1 Inhibitory effect of potassium SCN^- on NAP activity

Double-reciprocal plots ($1/v$ versus $1/[S]$) showing competitive inhibition by potassium SCN^-. (■) No inhibitor present. Inhibition was measured with [SCN^-] at 1 mM (●) and 10 mM (▲). Enzyme concentration was 0.1 μM in 20 mM Hepes, pH 7.2, at 30 °C. The reaction was started by the addition of nitrate, and the reoxidation of MV^+ was monitored at 600 nm. Each continuous line is the best fit where each point represents the mean ($n = 3$); the error was $< 5\%$ in each case.

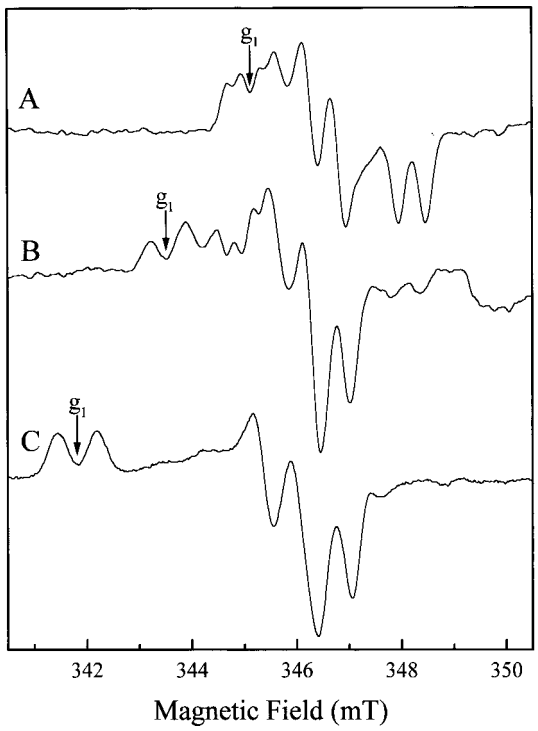

Figure 2 Mo(V) EPR signals of NAP

(**A**) High-*g* (resting); (**B**) High-*g* (thiocyanate) and (**C**) Very High-*g*. Enzyme concentrations were $\approx 300\ \mu$M in 20 mM Hepes, pH 7.2. Conditions of measurement: microwave frequency, 9.64 GHz; microwave power, 2 mW; modulation amplitude, 0.1 mT; temperature, 60 K.

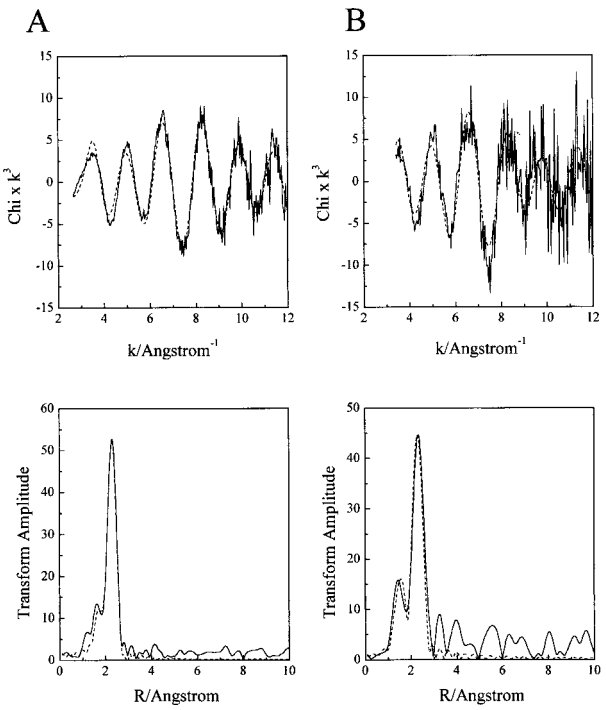

Figure 3 k^3-weighted EXAFS and Fourier transform of the Mo(IV) form of NAP with bound SCN^-

(**A**) Dithionite-reduced. Sample concentration was $\sim 600\ \mu$M in 20 mM Hepes, pH 7.2. (**B**) Dithionite-reduced plus SCN^-. The sample concentration was decreased to $\approx 400\ \mu$M in 20 mM Hepes, pH 7.2, by the addition of SCN^- to a final concentration of 10 mM.

inhibition. From these data, the observed K_i for SCN^- inhibition was determined to be 4.0 ± 0.6 mM. This type of inhibition suggests that both SCN^- and nitrate bind at the same site, thus it would seem likely that SCN^- is a direct ligand to the active-site Mo.

Effect of SCN^- on Mo(V) EPR after redox cycling

The High-*g* (resting) EPR signal can be detected in the 'as prepared' resting sample and accounts for 2.5–10 % of the total Mo (Figure 2A). It has rhombic character, but exhibits unusually low anisotropy (Table 1). The signal is split by two weakly interacting $I = 1/2$ nuclei, $A^1_{av} = 15.41$ MHz and $A^2_1 = 7.85$ MHz; the weaker splitting can only be detected in the g_1 region. A novel Mo(V) EPR signal could be generated in NAP by reducing the enzyme with dithionite, adding KSCN (10 mM), and then re-oxidizing with ferricyanide or air (Figure 2B). Addition of SCN^- to the 'as-prepared' enzyme did not affect the High-*g* (resting) EPR signal, suggesting that reduction of NAP to an Mo(IV) species was a prerequisite to SCN^- binding. The signal observed in the SCN^- treated samples has a g_{av} of 1.994 and displays Curie temperature-dependence. This new signal we have classified as an Mo(V) High-*g* signal and is subsequently referred to as the 'High-*g* (thiocyanate)' signal. It is also evident, particularly at higher field values, that a small percentage of the High-*g* (resting) signal remains detectable in this sample, indicating incomplete conversion into High-*g* (thiocyanate) species. Like the High-*g* (resting) signal, High-*g* (thiocyanate) is also split by weakly interacting $I = 1/2$ nuclei ($A_{av} = 17.66$ MHz; Table 1), which remained in spectra collected from enzyme exchanged into ^2H_2O buffer and probably arises due to a methylene proton of the co-ordinating cysteine ligand. EPR signals from the oxidized [3Fe–4S] cluster and haem *c* of the High-*g* (thiocyanate) sample were identical with those of samples containing High-*g* (resting) signals, demonstrating that SCN^- is not interacting with other redox centres within the enzyme. The EPR spectrum of the Very-High-*g* species of NAP formed by redox cycling in the presence of cyanide is included for comparison (Figure 3C).

Table 1 Representative EPR parameters for various signals of NAP

Signal	g_1	g_2	g_3	g_{av}	Anisotropy (g_1–g_3)	Rhombicity (g_1–g_2)/(g_1–g_3)	A_1 (MHz)	A_2 (MHz)	A_3 (MHz)	A_{av} (MHz)	Reference
High-*g* (resting)	1.998	1.990	1.980	1.989	0.018	0.46	17.93, 7.85*	14.57	14.01	15.41	This study [15]
High-*g* (thiocyanate)	2.008	1.991	1.985	1.994	0.023	0.74	18.78	18.50	15.41	17.66	This study
Very High-*g*	2.022	1.999	1.993	2.005	0.029	0.80	20.74	20.74	18.50	19.90	This study [15]

* Interaction with a second $I = 1/2$ nucleus in this species could be resolved only in the g_1 feature.

Table 2 Comparison of various fits to the EXAFS data of the nitrate reductase samples

n is the number of scatterers ± 20%; *r* is the Mo-scatterer distance ± 0.02 Å; $2\sigma^2$ is the Debye–Waller factor ± 20%. Fits shown in **bold** type represent the best fits obtained for each sample.

	Mo═O			Mo–O			Mo–S			
Sample and state	*n*	*r* (Å)	$2\sigma^2$ (Å^2)	*n*	*r* (Å)	$2\sigma^2$ (Å^2)	*n*	*r* (Å)	$2\sigma^2$ (Å^2)	Residual
Dithionite–reduced	**1**	**1.74**	**0.007**	**1**	**2.14**	**0.003**	**3**	**2.35**	**0.006**	**38.9**
	1	1.74	0.007	1	2.19	0.013	4	2.34	0.009	39.6
	1	1.73	0.008	–	–	–	3	2.34	0.005	40.2
	2	1.74	0.019	–	–	–	3	2.33	0.005	43.1
	1	1.73	0.007	–	–	–	5	2.34	0.011	43.6
	–	–	–	–	–	–	5	2.34	0.011	53.4
Dithionite–reduced + thiocyanate	**1**	**1.70**	**0.006**	–	–	–	**4**	**2.34**	**0.010**	**58.2**
	1	1.69	0.006	–	–	–	4	2.35	0.010	
							1	2.20	0.018	58.6
	1	1.70	0.005	–	–	–	5	2.34	0.013	58.6
	1	1.69	0.006	1	2.01	0.012	4	2.34	0.010	59.2
	1	1.69	0.006	1	2.00	0.016	3	2.33	0.006	59.6
	1	1.70	0.006	–	–	–	3	2.34	0.006	59.8
	2	1.69	0.009	–	–	–	4	2.34	0.010	61.7

EXAFS analysis of SCN^--treated NAP

The 'as prepared' NAP was reduced with a 50-fold excess of dithionite and incubated at room temperature for 10 min. EPR analysis revealed a decrease in intensity of the Mo(V) High-*g* (resting) signal to approx. 2.5% of the total Mo content; thus the sample was assumed to be 97.5% Mo(IV). The Mo(IV) K-edge EXAFS (Figure 3A) of the reduced sample was obtained and the data was best-fitted with one oxygen atom at 1.74 Å, one oxygen atom at 2.14 Å and three equivalent sulphur atoms at 2.35 Å (Table 2). This fit is consistent with the data obtained previously for dithionite-reduced samples [15]. To a sample of reduced NAP, KSCN was added to a final concentration of 10 mM and incubated for a further 10 min at room temperature. EXAFS analysis (Figure 3B) of the SCN^- bound sample was recorded, and the data fitted best with one oxygen atom at 1.70 Å and four sulphur atoms at 2.34 Å (Table 2). Attempts to fit the data with three sulphur atoms at the same distance, gave larger residuals (Table 2). Confirmation that Mo remained Mo(IV) upon the addition of SCN^- was obtained by monitoring the Mo K-edge position which remained at 20008 eV. The increase in sulphur co-ordination, in combination with the competitive inhibition by SCN^- and the generation of a novel Mo(V) High-*g* (thiocyanate) EPR species is taken as evidence for the direct binding of SCN^- via the sulphur atom to the Mo(IV) species of NAP.

DISCUSSION

In the present paper the effect of KSCN as an inhibitor of the periplasmic nitrate reductase (NAP) from *P. pantotrophus* has been investigated. Results are presented that show NAP is sensitive to SCN^- inhibition, with SCN^- acting as a competitive inhibitor of nitrate. The observed K_i of $\approx$ 4.0 mM for SCN^- inhibition is slightly lower than that reported for the competitive inhibition by the azide anion ($K_i \approx 11$ mM) [15], but again demonstrates that NAP from *P. pantotrophus* is poorly sensitive to anionic inhibition. Analysis of the Mo K-edge EXAFS of the dithionite-reduced NAP was best-fitted as a mono-oxo Mo(IV) species with three Mo–S ligands at 2.35 Å and an Mo–O ligand at 2.14 Å, in agreement with previous results [15]. The three sulphur ligands must arise from the co-ordinating cysteine ligand and one pterin dithiol. Thus the second pterin has dissociated from Mo under these reducing conditions. We have suggested previously that the possible lability of one of the pterin dithiolene ligands may play an important role in catalysis by allowing substrate binding and/or modulating redox potential [15]. The addition of SCN^- to reduced Mo(IV) NAP generated a sample that was best fitted as a mono-oxo (1.70 Å) Mo(IV) species with four Mo–S ligands at 2.34 Å. The additional sulphur ligand at 2.34 Å may be taken as evidence for the direct binding of SCN^- to Mo(IV). It should be noted that attempts to fit three sulphur ligands plus a long bond (2.00 Å) oxygen/nitrogen produced a significantly worse fit. Thus it would appear that, given the option of SCN^- forming a bond via the nitrogen (Mo(IV)–NCS) or via the sulphur (Mo(IV)–SCN), that the sulphur provides the favoured Mo ligand.

EPR analysis has revealed the formation of a novel Mo(V) EPR spectrum upon redox cycling in the presence of SCN^-. Because the Mo(V) High-*g* (thiocyanate) species only represents approx. $\approx$ 10% of the sample, no direct evidence from EXAFS for either the co-ordination geometry or sulphur co-ordination number can be obtained and, as a consequence, we can only speculate as to the likely co-ordination sphere of the Mo(V) High-*g* (thiocyanate) species. The EPR spectrum for the SCN^- sample is interesting, since it displays a g_{av} value higher than that of the Mo(V) High-*g* (resting) signal. The most common change in the Mo co-ordination sphere that gives rise to such g_{av} shifts is variation in the number of sulphur ligands, and a correlation between increasing sulphur co-ordination and increasing g_{av} value has also been reported for studies on model compounds [16,17]. Similarly, a decrease in g_{av} accompanies the Mo–SH-to-Mo–OH transition seen in molybdopterin-containing hydroxylases [17]. However, an alternative explanation for elevated g_{av} values might involve conformational changes around the Mo centre. Such changes appear to be induced by cyanide binding to NAP. In this case, cyanide is a non-competitive inhibitor of NAP and does not bind at the Mo atom [15]. EXAFS analysis suggests that the binding of cyanide within the active-site pocket causes a change in the Mo co-ordination geometry. This results in a significant distortion of the bond lengths of the co-ordinating pterin sulphur ligands that may lead to an increase in the observed g_{av}.

The combined evidence of (i) the competitive nature of SCN^- inhibition of periplasmic nitrate reductase activity, (ii) the

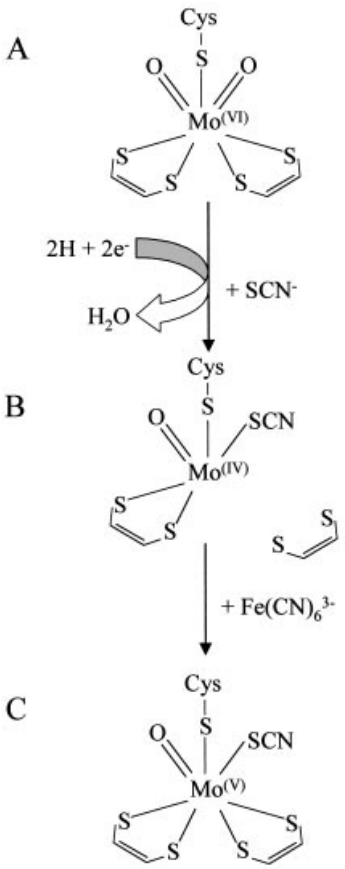

Scheme 1 Model for the binding of SCN^- to Mo(IV) of NAP

(**A**) 'As prepared' oxidized Mo(VI) NAP. (**B**) Dithionite reduced to Mo(IV) and binding of SCN^-. (**C**) Predicted structure of Mo(V) High-*g* (thiocyanate) species following oxidation by ferricyanide.

increase in sulphur co-ordination of Mo(IV) upon SCN^- binding and (iii) the elevated Mo(V) EPR g_{av} value following redox cycling in the presence of SCN^- makes a compelling argument that the Mo(V) High-*g* (thiocyanate) species is co-ordinated by an additional sulphur ligand rather than the SCN^-, inducing changes in the Mo-pterin co-ordination geometry. We have shown previously that the Mo(V) High-*g* (resting) species is completely insensitive to changes in pH and the binding of exogenous ligands [15]. On the basis of these observations we have considered it unlikely that the Mo(V) High-*g* (resting) species has any vacant co-ordination sites and have therefore suggested that it is co-ordinated by five sulphur ligands – four provided by the two pterins and a fifth sulphur ligand from a co-ordinating cysteine ligand (Cys^{181}). Given that the novel Mo(V) High-*g* (thiocyanate) EPR species has a g_{av} value of 1.994 compared with the g_{av} of 1.989 for the High-*g* (resting), we suggest that this species may be co-ordinated by six sulphur ligands – four provided by the two pterins, one from Cys^{181} and one from the co-ordinated SCN^- (Scheme 1).

The observation of the direct binding of exogenous sulphur ligands to the molybdopterin cofactor of NAP may have implications for the mechanism of sulphur reduction by the Mo-containing enzymes that are involved in tetrathionate and thiosulphate respiration [19]. On the basis of the results presented herein, the direct binding of tetrathionate to the Mo(IV) form of tetrathionate reductase, via a sulphur atom would seem likely. With tetrathionate bound to Mo(IV), the oxidation of Mo(IV) to Mo(VI) would then result in the two-electron reductive cleavage of the tetrathionate sulphur–sulphur bond, forming two molecules of thiosulphate ($S–SO_3^-$).

In conclusion, these results have demonstrated, for the first time, that the periplasmic nitrate reductase from *P. pantotrophus* is inhibited by high concentrations of KSCN. The formation of the novel EPR Mo(V) High-*g* (thiocyanate) species with elevated *g*-values upon redox cycling in the presence of SCN^-, and the presence of an additional sulphur ligand at 2.34 Å in the co-ordination sphere of the Mo(IV) SCN^- bound species suggest that SCN^- binds directly to Mo(IV) through a sulphur ligand. These results further demonstrate that the catalytically active site of NAP is flexibly with the Mo able to accommodate variability in the nature and number of the ligands to which it is attached. Furthermore, the ability to generate an SCN^--bound form of Mo(IV) may prove useful as a probe for the understanding of sulphur-atom-transfer reactions catalysed by MGD-containing enzymes.

This work was supported by Biotechnology and Biological Sciences Research Council grant GrCO8666 to D. J. R., B. C. B., A. J. T. and S. J. F., and grant BO3032-1 to the Centre for Metalloprotein Spectroscopy and Biology, University of East Anglia, and an Engineering and Physical Sciences Research Council grant to C. D. G., J. M. C. and D. J. R. for provision of Synchrotron beam-time. We are grateful to Mr David Clarke and Mr Jeremy Thornton for help with the growth of *P. pantotrophus* and the purification of NAP.

REFERENCES

1 Sears, H. J., Little, P. J., Richardson, D. J., Spiro, S., Berks, B. C. and Ferguson, S. J. (1997) Identification of an assimilatory nitrate reductase in mutants of *Paracoccus denitrificans* GB17 deficient on nitrate respiration. Arch. Microbiol. **167**, 61–66
2 Berks, B. C., Ferguson, S. J., Moir, J. W. B. and Richardson, D. J. (1995) Enzymes and associated electron transport systems that catalyse the respiratory reduction of nitrogen oxides and oxyanions. Biochim. Biophys. Acta **1232**, 97–173
3 Ludwig, W., Mittenhuber, G. and Freidrich, C. G. (1993) Transfer of *Thiosphaera pantotropha* to *Paracoccus denitrificans*. Int. J. Syst. Bacteriol. **43**, 363–367
4 Berks, B. C., Richardson, D. J., Reilly, A., Willis, A. C. and Ferguson, S. J. (1995) The *napEDABC* gene cluster encoding the periplasmic nitrate reductase system of *Thiosphaera pantotropha*. Biochem. J. **309**, 983–992
5 Berks, B. C., Richardson, D. J., Robinson, C., Reilly, A., Aplin, R. T. and Ferguson, S. J. (1994) Purification and characterization of the periplasmic nitrate reductase from *Thiosphaera pantotropha*. Eur. J. Biochem. **220**, 117–124
6 Breton, J., Berks, B. C., Reilly, A., Thomson, A. J., Ferguson, S. J. and Richardson, D. J. (1994) Characterisation of the paramagnetic iron-containing redox centres of *Thiosphaera pantotropha* periplasmic nitrate reductase. FEBS Lett. **345**, 76–80
7 Richardson, D. J., Sears, H. J., Berks, B. C., Ferguson, S. J and Spiro, S (1997) The bacterial nitrate reductases. In Advances en el Metabolismo del Nitrogeno: de la Fistologia a la Biologia Molecular (Vega, J. M., Pedro, J. A., Castillo, F. and Maldonado, J. M., eds.), pp. 565–574, Secretariado de Publicaciones de la Universidad de Sevilla, Porvenir, Sevilla, Spain
8 Dias, J. M., Than, M. E., Humm, A., Huber, R., Bourenkov, G. P., Bartunik, H. D., Bursakov, S., Calvete, J., Caldeira, J., Carneiro, C. et al. (1999) Crystal structure of the first dissimilatory nitrate reductase at 1.9 Å solved by MAD methods. Structure **7**, 65–789
9 Schindelin, H., Kisker, C., Hilton, J., Rajagopalan, K. V. and Rees, D. C. (1996) Crystal structure of DMSO reductase: redox-linked changes in molybdopterin coordination. Science (Washington, D.C.) **272**, 1615–1621
10 Schneider, F., Löwe, J., Huber, R., Schindelin, H., Kisker, C. and Knäblein, J. (1996) Crystal structure of dimethyl sulfoxide reductase from *Rhodobacter capsulatus* at 1.88 Å resolution. J. Mol. Biol. **263**, 53–69
11 McAlpine, A. S., McEwan, A. G., Shaw, A. L. and Bailey, S. (1997) Mo active centre of DMSO reductase from *Rhodobacter capsulatus:* crystal structure of the oxidised enzyme at 1.82 Å resolution and the dithionite-reduced enzyme at 2.8 Å resolution. J. Biol. Inorg. Chem. **2**, 690–701
12 Boyington, J. C., Gladyshev, V. N., Khangulov, S. V., Stadtman, T. C. and Sun, P. D. (1997) Crystal structure of formate dehydrogenase H: catalysis involving Mo, molybdopterin, selenocysteine and an Fe4S4 cluster. Science (Washington, D.C.) **275**, 1305–1308

13 Czjzek, M., Dos Santos, J. P., Pommier, J., Giordano, G., Méjean, V. and Haser, R. (1998) Crystal structure of oxidized trimethylamine N-oxide reductase from *Shewanella massilia* at 2.5 Å resolution. J. Mol. Biol. **284**, 435–447
14 Bennett, B., Benson, N., McEwan, A. G. and Bray, R. C. (1994) Multiple states of the Mo centre of dimethylsulphoxide reductase from *Rhodobacter capsulatus* revealed by EPR spectroscopy. Eur. J. Biochem. **225**, 321–331
15 Butler, C. S., Charnock, J. M., Bennett, B., Sears, H. J., Reilly, A. J., Ferguson, S. J., Garner, C. D., Lowe, D. J., Thomson, A. J., Berks, B. C. and Richardson, D. J. (1999) Models for molybdenum coordination during the catalytic cycle of periplasmic nitrate reductase from *Paracoccus denitrificans* derived from EPR and EXAFS spectroscopy. Biochemistry **38**, 9000–9012
16 Chang, C. S. J., Collison, D., Mabbs, F. E. and Enemark, J. H. (1990) Synthesis and characterisation of mononuclear oxoMo(V) complexes with aliphatic diolato, dithiolato, or alkoxo ligands: effect of chelate ring size on the properties of the metal center. Inorg. Chem. **29**, 2261–2267
17 Dowerah, D., Spence, J. T., Singh, R., Wedd, A. G., Wilson, G. L., Farchione, F., Enemark, J. H., Kristofzki, J. and Bruck, M. (1987) Mo(VI) and Mo(V) complexes with *N,N′*-dimethyl-*N,N′*-bis(2-mercaptophenyl)ethylenediamine – electrochemical and electron-paramagnetic resonance models for the Mo(VI/V) centers of the Mo hydroxylases and related enzymes. J. Am. Chem. Soc. **109**, 5655–5665
18 Gangeswaran, R., Lowe, D. J. and Eady, R. R. (1993) Purification and characterization of the assimilatory nitrate reductase for *Azotobacter vinelandii*. Biochem. J. **289**, 335–342
19 Hensel, M., Hinsley, A. P., Nikolaus, T., Sawers, G. and Berks, B. C. (1999) The genetic basis of tetrathionate respiration in *Salmonella typhimurium*. Mol. Microbiol. **32**, 275–287
20 Craske, A. L. and Ferguson, S. J. (1986) The respiratory nitrate reductase from *Paracoccus denitrificans*. Molecular characterisation and kinetic properties. Eur. J. Biochem. **158**, 429–436
21 Bennett, B., Berks, B. C., Ferguson, S. J., Thomson, A. J. and Richardson, D. J. (1994) Mo(V) electron paramagnetic resonance signal from the periplasmic nitrate reductase of *Thiosphaera pantotropha*. Eur. J. Biochem. **226**, 789–798
22 Binsted, N. (1998) EXCURV98 program, Central Laboratory of the Research Councils, Daresbury Laboratory, Warrington
23 Lee, P. A. and Pendry, J. B. (1975) Theory of the extended x-ray absorption fine structure. Phys. Rev. **B11**, 2795–2811
24 Gurman, S. J., Binsted, N. and Ross, I. (1984) A rapid, exact, curved-wave theory for EXAFS calculations. J. Phys. **C17**, 143–151
25 Hedin, L. and Lundqvist, S. (1969) Effects of electron–electron and electron–phonon interactions on the one-electron states of solids. Solid State Phys. **23**, 1–181

Received 26 June 2000/4 September 2000; accepted 4 October 2000